Journal of Alloys and Compounds 508 (2010) 546–553

Contents lists available at ScienceDirect

Journal of Alloys and Compounds

journal homepage: www.elsevier.com/locate/jallcom

Effect of Dy_2O_3 on the structure and electrical properties of $(Bi_{0.5}Na_{0.5})_{0.94}Ba_{0.06}TiO_3$ lead-free piezoelectric ceramics

Peng Fu*, Zhijun Xu, Ruiqing Chu, Wei Li, Qian Xie, Yanjie Zhang, Qian Chen

Institute of Materials Science and Engineering, Liaocheng University, Liaocheng 252059, PR China

ARTICLE INFO

Article history:
Received 27 May 2010
Received in revised form 25 August 2010
Accepted 25 August 2010

Keywords:
Dy_2O_3-doped
BNBT6 ceramics
Piezoelectric property
Ferroelectric property
Dielectric property

ABSTRACT

Dy_2O_3 (0–0.8 wt.%)-doped $(Bi_{0.5}Na_{0.5})_{0.94}Ba_{0.06}TiO_3$ (abbreviated as BNBT6) lead-free piezoelectric ceramics were synthesized by conventional solid-state processes. The compositional dependence of phase structure and electrical properties of the ceramics was studied. X-ray diffraction (XRD) data shows that 0.2–0.8 wt.% Dy_2O_3 can diffuse into the lattice of BNBT6 ceramics and forms a pure perovskite phase. SEM images indicate that all the modified ceramics have a clear grain boundary and a uniformly distributed grain size, and the BNBT6 ceramics doped with appropriate Dy_2O_3 become denser. At room temperature, the ceramics doped with 0.6 wt.% Dy_2O_3 have the highest piezoelectric constant (d_{33} = 170 pC/N), higher mechanical quality factor (Q_m = 102), high relative dielectric constant (ε_r = 1611) and lower dissipation factor ($\tan\delta$ = 0.051) at a frequency of 10 kHz. The BNBT6 ceramics doped with 0.4 wt.% Dy_2O_3 have the highest planar coupling factor (k_p = 0.33). Moreover, all BNBT6-x (wt.%) Dy_2O_3 ceramics exhibit a typical relaxor behavior with diffuse phase transition characteristics and the degree of ferroelectric relaxation behavior attains peak value at doping level of 0.4 wt.%.

1. Introduction

Most piezoelectric ceramic devices such as filters, resonators, actuators, sensors, and so on, were fabricated by using lead-based piezoelectric ceramic materials such as $Pb(Zr,Ti)O_3$ (PZT) and PZT based multi-component ceramics due to their superior piezoelectric properties [1–3]. However, the preparation and application of lead-based ceramics has not only caused serious lead pollution and environmental problems, but also led to instability of the composition owing to its high volatility during sintering [4,5]. Multinational governments like the European Union have enacted laws to ban the use of lead in the manufacture of many products [6]. Therefore, lead-free piezoelectric ceramics have attracted considerable attention as new substituting materials for lead-based ceramics.

$Bi_{0.5}Na_{0.5}TiO_3$ (BNT) is well known as a complex ABO_3 perovskite ceramic with a ferroelectric rhombohedral phase at room temperature and shows a great prospect not only for environment protection but also for various applications. However, the shortcoming of BNT ceramics is its high conductivity and high coercive field

(E_c = 7.3 kV/mm), and pure BNT is difficult to be poled and cannot be a good piezoelectric material [7–11].

To improve the poling process and enhance the piezoelectric properties of the BNT ceramics, a number of BNT-based solid solutions, such as BNT-$BaTiO_3$ [12,13], BNT-$(Ba,Sr)TiO_3$ [14], BNT-$Bi_{0.5}K_{0.5}TiO_3$ [15], BNBT-$Ba(Zr_{0.04}Ti_{0.96})O_3$ [10], BNT-$SrTiO_3$-$Bi_{0.5}Li_{0.5}TiO_3$ [16], BNT-$Bi_{0.5}K_{0.5}TiO_3$-$Bi_{0.5}Li_{0.5}TiO_3$ [17], BNT-$Bi_{0.5}K_{0.5}TiO_3$-$BiFeO_3$ [18] and Bi_2O_3 doped BNT-$BaTiO_3$ [19] have been developed and studied in recent years.

Among the BNT systems that have been developed so far, $(Na_{0.5}Bi_{0.5})_{1-x}Ba_xTiO_3$ [$(1-x)$BNT–xBT] system seems more interesting due to the existence of a trigonal–tetragonal morphotropic phase boundary (MPB) near x = 0.06 [20–22]. When tetragonal and trigonal system exists simultaneously, electric domain wall turns easily, increasing spontaneous polarization intensity greatly and remnant polarization, which can provide substantially excellent piezoelectric properties [23–25]. So, BNBT6 ceramics exhibit relatively higher piezoelectric properties and are regarded as an excellent candidate for lead-free piezoelectric ceramics to replace lead-based piezoelectric ceramics.

However, for practical applications, the piezoelectric properties of BNBT6 ceramics need to be further enhanced. To improve their piezoelectric properties further, rare earth oxides are often used as the additive in prepared the BNBT6 ceramics. Several kinds of rare earth oxide such as CeO_2 [26–28], Y_2O_3 [29], and La_2O_3 [30] have been tested to further modify piezoelectric properties of BNBT6 ceramics, and the addition of these rare earth oxides has a prominent influence on the structure and electrical properties of the BNBT6 ceramics. However, the research of Dy_2O_3 doped BNBT6 ceramics has not been reported so far. As we all know, the radius of Dy^{3+} (0.912 Å) is very close to the radius of Bi^{3+} (1.03 Å) and Na^+ (1.02 Å). In view of the radius, it is possible for Dy^{3+} to enter into

* Corresponding author.
E-mail addresses: fupeng9806@126.com, fupeng9898@yahoo.cn (P. Fu).

0925-8388/$ – see front matter © 2010 Elsevier B.V. All rights reserved.
doi:10.1016/j.jallcom.2010.08.117

the A-sites of BNBT6 perovskite and affect the properties of BNBT6 ceramics. Therefore, in present work, Dy_2O_3 was selected as dopant of BNBT6 ceramics and the influences of Dy_2O_3 on the structure and electrical properties of BNBT6 ceramics were studied.

In this work, the MPB phase of the BNBT6 ceramics was identified, and the compositional dependence of phase structure and the electrical properties of the BNBT6 ceramics were studied. The results demonstrated that the appropriated Dy_2O_3 doped BNBT6 ceramics possessed enhanced electrical properties.

2. Experimental details

Dy_2O_3 doped BNBT6 ceramics were prepared by conventional solid-state reaction processes. The oxide or carbonate powders of high purity Bi_2O_3 (99.63%), Na_2CO_3 (99.5%), $BaCO_3$ (99.5%), TiO_2 (99.5%) and Dy_2O_3 (99.9%) powders were used as the raw materials.

Firstly, the powders of these raw materials were mixed together by a planet mill in a nylon jar with agate ball for 10 h. Next, the mixed powders were dried and calcined at 900 °C for 2 h; the major reaction is as follows:

$$0.235Bi_2O_3 + 0.235Na_2CO_3 + 0.06BaCO_3 + TiO_2 \rightarrow (Bi_{0.5}Na_{0.5})_{0.94}Ba_{0.06}TiO_3 + 0.295CO_2 \uparrow \quad (1)$$

After calcining, the powders were ball-milled again by the planet mill with agate balls for 4 h, the dried powders were mixed with polyvinyl alcohol (PVA) and pressed into disks with a diameter of 12 mm, and then calcined at 800 °C to exclude binder (PVA). Finally, the pressed disks were sintered at 1150 °C for 2 h in air. The sintered samples were polished and pasted with silver slurry on both faces, and then fired at 740 °C as electrodes. Specimens for piezoelectric measurements were poled for 20 min by silicone oil bath with the existence of a dc electric field of 4–5 kV/mm. After laying the polarized specimens for approximate 24 h to release the remnant stress, piezoelectric properties were measured subsequently.

The density of sintered ceramics was measured by the Archimedes method. The crystal structure of BNBT6 ceramics was determined by X-ray diffraction (XRD) using a Cu K_α radiation ($\lambda = 1.54178$ Å) (D8 Advance, Bruker Inc., Germany). The microstructure of the sintered ceramics was observed by scanning electron microscope (SEM; JSM-5900, Japan). The piezoelectric coefficient d_{33} was measured using a quasistatic d_{33}-meter (YE2730, SINOCERA, China). The electro-mechanical coupling factors k_p, the mechanical quality factor Q_m were determined by a resonance–antiresonance method on the basis of IEEE standards using an Agilent 4294A impedance analyzer. And the curve between relative dielectric constant and temperature were also measured by precision impedance analyzer (Agilent 4294A, America). The room temperature ferroelectric polarization versus electric field (P–E) measurements was using a standardized ferroelectric test system (TF2000, Germany) with an applied field of 5.5–7.0 kV/mm.

3. Results and discussion

Fig. 1 shows the XRD patterns of BNBT6-x (wt.%) Dy_2O_3 ($x = 0.0$, 0.2, 0.4, 0.6, 0.8) ceramics sintered at 1150 °C in the 2 θ range of 20–70°. From Fig. 1, it is indicated that all specimens exhibit typical ABO_3 perovskite diffraction peaks and no second phases are observed, meaning that Dy^{3+} may have completely entered into crystalline lattice structure of BNBT6 ceramics to form a homologous solid solution or the second phase can not be detected because of the small doping amount of Dy_2O_3. The magnification of Fig. 1 in the 2θ ranges of (A) 39–41° and (B) 46–47° is shown in Fig. 2. Obvious splitting of XRD peaks is detected for all specimens, as shown in Fig. 2. They can be assigned to a (0 0 3)/(0 2 1) peak splitting at about 40° and a (0 0 2)/(2 0 0) peak splitting at about 46.5° according to a rhombohedral symmetry and a tetragonal symmetry, respectively. It is shown that two phases of rhombohedral and tetragonal coexist, and suggests that a morphotropic phase boundary (MPB) between the rhombohedral and tetragonal phases exists in all samples. These results indicate that the addition of Dy_2O_3 does not lead to an obvious change in the phase structure.

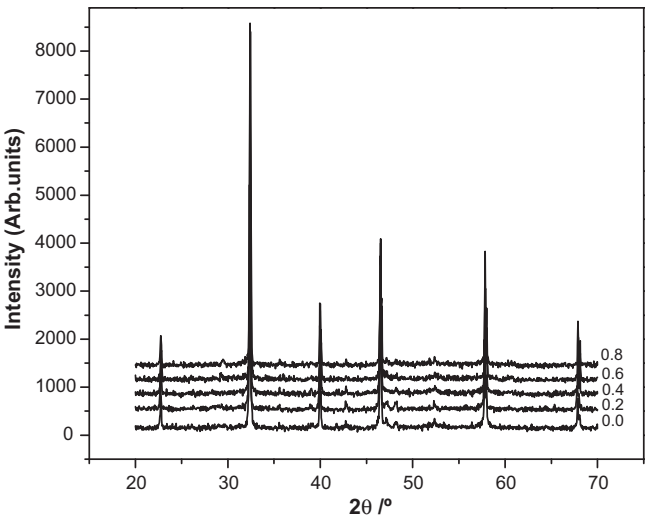

Fig. 1. XRD patterns of BNBT6-x (wt.%) Dy_2O_3 ($x = 0.0$–0.8) ceramics.

The SEM micrographs of the surface and fracture surface of the BNBT6-x (wt.%) Dy_2O_3 ceramics are shown in Figs. 3 and 4, respectively. For the pure BNBT6 ceramics, the grain sizes are not very homogeneous, and some distinct pores exist in the grain boundary are observed, whereas, the average grain size vary significantly with an increase in the Dy_2O_3 content, as shown in Fig. 3. Compared with the pure BNBT6 ceramics with an average grain size of 2 μm, the average grain size of the BNBT6 ceramics doped with

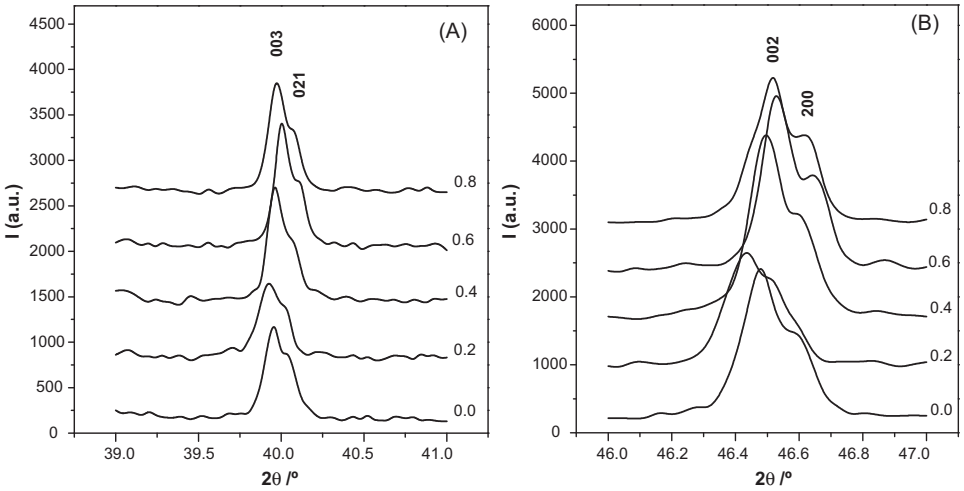

Fig. 2. Magnification of XRD patterns in the 2θ ranges of (A) 39–41° and (B) 46–47°.

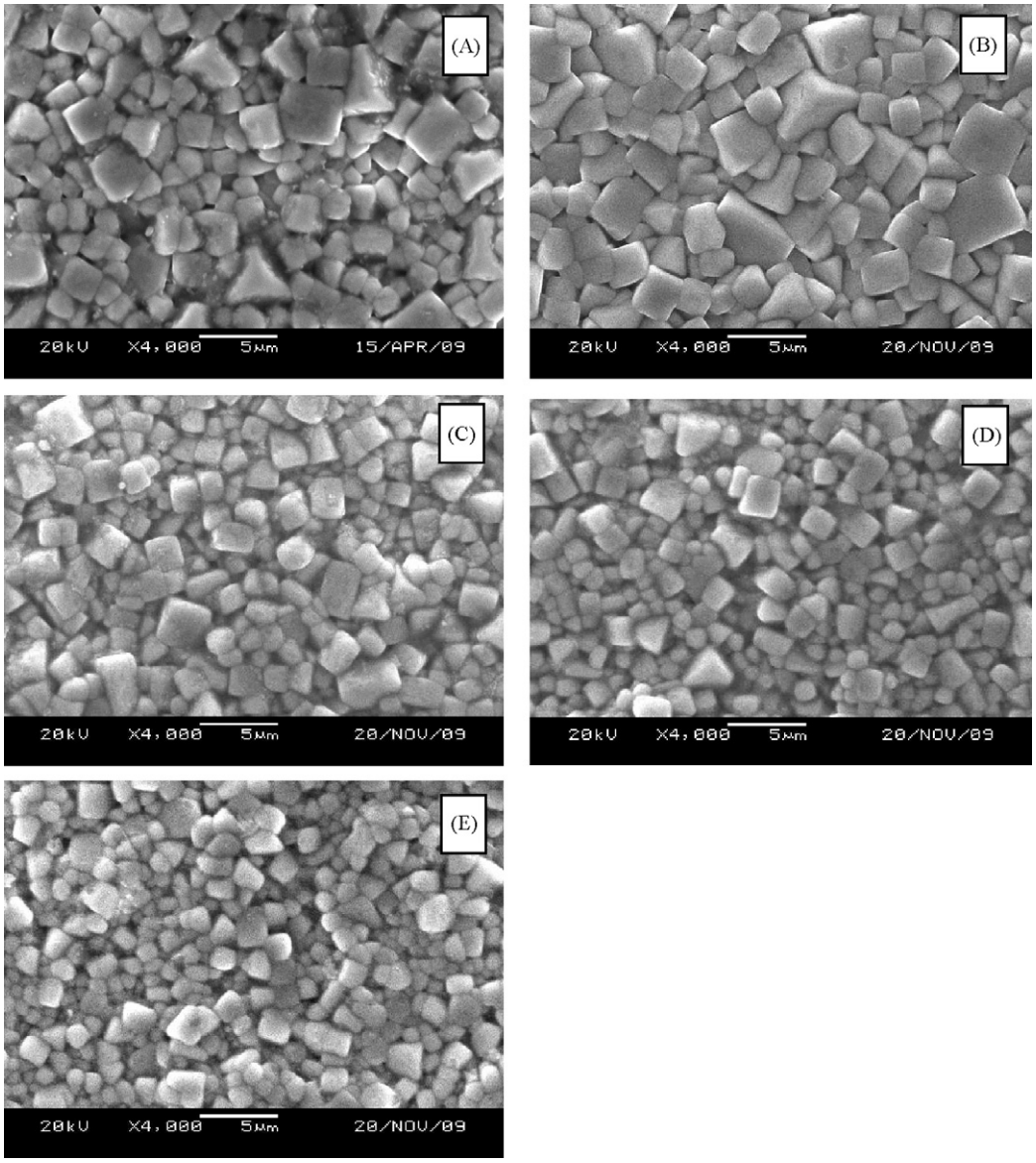

Fig. 3. SEM micrographs of surfaces for BNBT6-x (wt.%) Dy_2O_3 ceramics sintered at 1150 °C: (A) $x = 0.0$, (B) $x = 0.2$, (C) $x = 0.4$, (D) $x = 0.6$, (E) $x = 0.8$.

0.2 wt.% Dy_2O_3 changes not obviously. However, further doping of Dy_2O_3 (0.4–0.8 wt.%) inhibits the grain growth and leads to the decrease of crystalline grains obviously. As is well known, the segregation of the oxide additive near grain boundaries decreases their mobility. The reduction in the mobility of the grain boundary weakens the mass transportation. As a result, grain growth is inhibited [31,32]. Moreover, it should be noticed that all the modified ceramics have a clear grain boundary and a uniformly distributed grain size, and the BNBT6 ceramics doped with Dy_2O_3 become denser obviously compared with pure BNBT6 ceramics. Piezoelectric ceramics usually require a high mechanical strength; the uniform grain microstructure is able to enhance the mechanical strength of piezoelectric ceramics [15]. Therefore, the ceramics with a homogeneous microstructure are advantageous for piezoelectric ceramics applications.

As shown in Fig. 4, in the present system the fractures of the ceramics are mainly transgranular. Furthermore, it is found that some pores exist in each specimen. The quantity of pores decreases and size of pores reduces, and the samples also become denser gradually as x increases from 0 to 0.6, demonstrating the usefulness of appropriate Dy_2O_3 as a sintering aid. However, excess Dy_2O_3 (0.8 wt.%) makes the porosity increase and the size of pores becomes big again.

The bulk density gradually increases as x increases from 0 to 0.6 and reaches a maximum value at $x = 0.6$. Then, the bulk density decreases with further increasing x to 0.8, as shown in Table 1. When $x = 0.6$, the samples possesses the maximum density of 5.87 g/cm^3, which is about 98.0% of the theoretical value. The densities of other ceramics are in the range of 5.58–5.74 g/cm^3, corresponding to the relative densities 93.2–96.8% of the theoretical value. These results indicate that the optimum Dy_2O_3 addition can promote sintering and thus improve the density of BNBT6 ceramics. However, excess Dy_2O_3 addition can also result in the decrease of the bulk density. The results agree with the results in Figs. 3 and 4.

The polarization versus electric field hysteresis loops of BNBT6-x (wt.%) Dy_2O_3 ceramics were measured at 10 Hz, and the results are presented in Fig. 5. It is evident that the ferroelectric properties of BNBT6 ceramics have significantly been affected by doping with Dy_2O_3. Compared with the pure BNBT6 ceramics, the remnant polarization P_r increases with increasing x and then decreases, giving a maximum value of 42.2 μC/cm^2 at $x = 0.4$. The coercive field E_c increases slightly with x increasing to 0.4 firstly, and then decreases

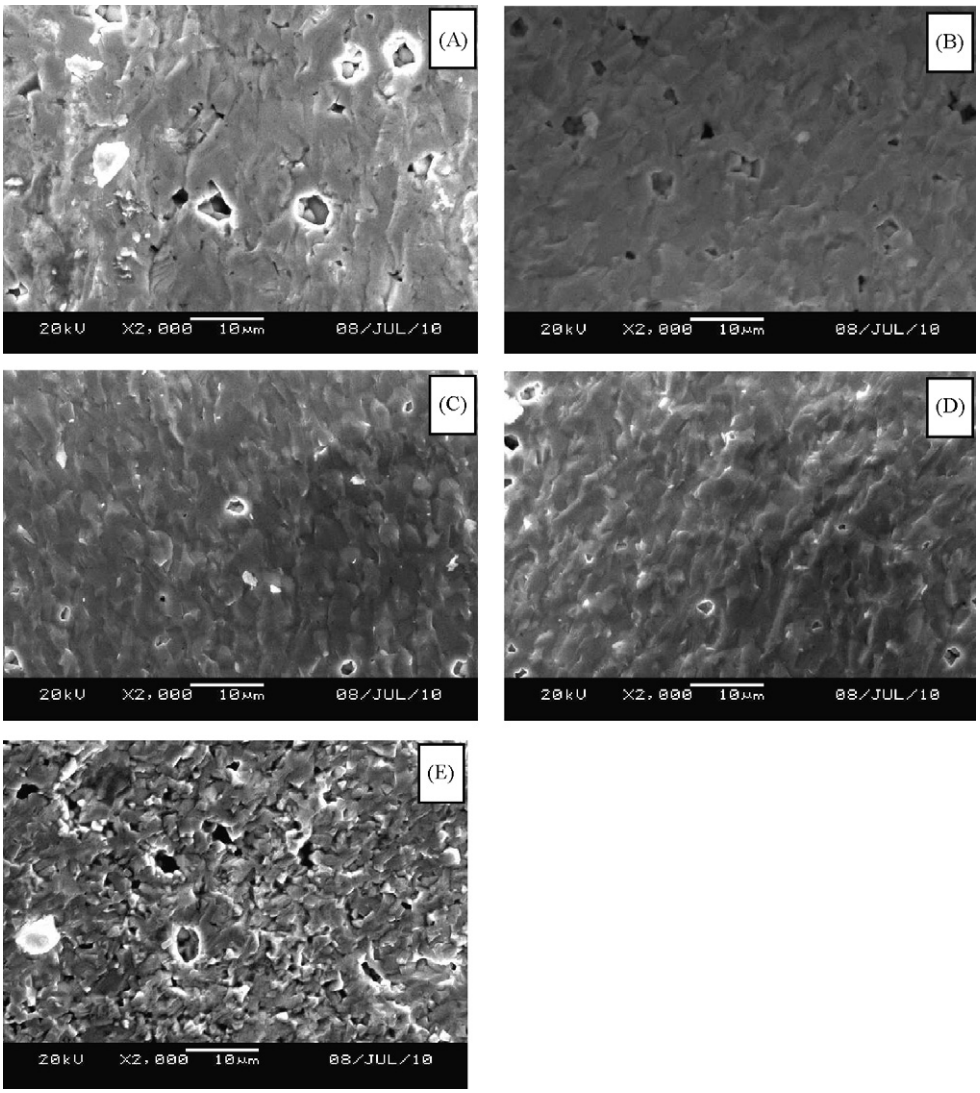

Fig. 4. SEM micrographs of the freshly fractured surfaces of BNBT6-x (wt.%) Dy_2O_3 ceramics: (A) $x = 0.0$, (B) $x = 0.2$, (C) $x = 0.4$, (D) $x = 0.6$, (E) $x = 0.8$.

gradually to 3.51 kV/mm with x further increasing to 0.8. This result indicates that the BNBT6 ceramics doped with appropriate Dy_2O_3 become "softer", with its specimens showing a larger remnant polarization P_r and a lower coercive field E_c [33]. Enhanced remnant polarization shows that ferroelectric properties of the BNBT6 ceramics have been improved with the addition of Dy_2O_3.

Moreover, the ferroelectric characteristic of the ceramics can also be assessed with the hysteresis loop squareness R_{sq}, which is typically understood to be ratio of P_r/P_s, where P_r is the remnant polarization at zero electric field and P_s is the saturated polarization obtained at some finite field strength below the dielectric breakdown. One can also use the loop squareness to measure not only the deviation in the polarization axis but also that in the electric field axis with the empirical expression, $R_{sq} = (P_r/P_s) + (P_{1.1Ec}/P_r)$

Table 1
Physical properties of specimen with the amount of Dy_2O_3 addition.

Dy_2O_3 (wt.%)	Density (g/cm^3)	d_{33} (pC/N)	k_p	Q_m	R_{sp}
$x = 0.0$	5.58	147	0.27	143	1.15
$x = 0.2$	5.71	148	0.31	132	1.40
$x = 0.4$	5.80	157	0.33	108	1.29
$x = 0.6$	5.87	170	0.28	102	1.28
$x = 0.8$	5.71	151	0.26	126	1.07

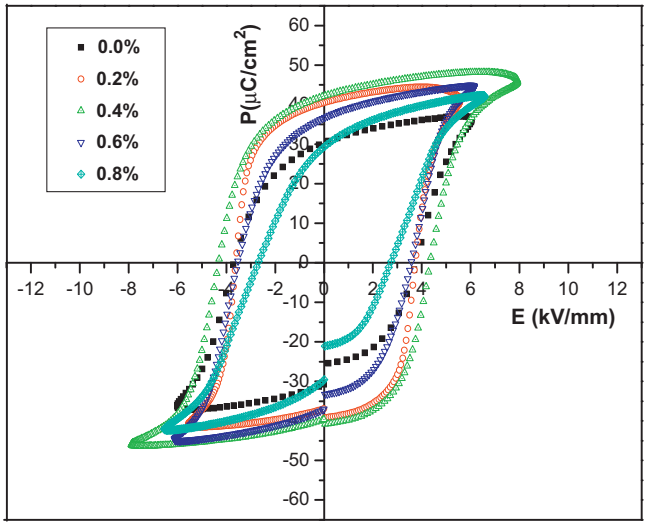

Fig. 5. Measured P–E hysteresis loops of BNBT6 ceramics with different amount of Dy_2O_3 additive sintered at 1150 °C.

where $P_{1.1Ec}$ is the polarization at the field equal to $1.1E_c$. For the ideal square loop, R_{sq} is equal to 2.00 [34]. The R_{sq} parameter lists in Table 1 for all BNBT6 ceramics at room temperature, the result shows that more loop squareness increases with increasing Dy_2O_3 contents firstly, and then decreases, and R_{sq} reaches a peak value (1.40) at $x = 0.2$. The square type loops are due to abruptly switching of a domain structure with an electric field. On the other hand, the slim type loops are owing to more sluggish reversal [34]. Increasing loop squareness can also show that the movement of domains becomes easier and the ferroelectric properties of the BNBT6 ceramics have been improved with the addition of Dy_2O_3.

Table 1 collects various room-temperature properties of BNBT6-x (wt.%) Dy_2O_3 ceramics sintered at 1150 °C. It was reported that the piezoelectric constant d_{33} of BNBT6 ceramics prepared by the conventional solid-state method attains about 120pC/N [10,22,35]. In our study, the pure BNBT6 ceramics has a relatively lager d_{33} of 147 pC/N, which is significantly larger than the reported values. As listed in Table 1, with the increasing value of x, the piezoelectric constant and planar coupling factor gradually increases firstly and reaches peak values at the doping level of 0.6 wt.% and 0.4 wt.% Dy_2O_3 respectively: $d_{33} = 170$ pC/N, $k_p = 0.33$, and then the two values decreases with the further increase of Dy_2O_3. The results show that the addition of appropriate Dy_2O_3 improves the piezoelectric properties of the BNBT6 ceramics significantly.

The variation of piezoelectric properties can be explained with the "soft" and "hard" additive model. According to "soft" and "hard" additive model [36], the radius of Dy^{3+} (0.912 Å) is very close to the radius of Bi^{3+} (1.03 Å) and Na^+ (1.02 Å). It is difficult for Dy^{3+} to enter into the B-sites of BNBT6 perovskite because of the smaller radius of Ti^{4+} (0.68 Å). Accordingly, Dy^{3+} is considered to be a substitute occupying the A sites of BNBT6 lattice. In the present study, the A-site (Bi^{3+} and Na^+) substitution by Dy^{3+} in BNBT6 ceramics can be formulated using defect chemistry expressions as:

$$Dy_2O_3 \xrightarrow{(Bi_{0.5}Na_{0.5})_{0.94}Ba_{0.06}TiO_3} 2Dy_{Bi} + 3O_O \quad (2)$$

$$Dy_2O_3 \xrightarrow{(Bi_{0.5}Na_{0.5})_{0.94}Ba_{0.06}TiO_3} 2Dy_{Na}^{\bullet\bullet} + 4V'_{NA} + 3O_O \quad (3)$$

When Dy^{3+} occupies Bi-site, as shown in Eq. (2), the substitution of Bi^{3+} by Dy^{3+} may cause the slack of BNBT6 lattice. The lattice deformation can make the ferroelectric domains reorientation more easily during electrical poling and leads to the enhancement of piezoelectric properties. Additionally, Dy^{3+} can also occupy the A-site of Na^+, as shown in Eq. (3). In this case, the valence of Dy^{3+} ion is higher than that of Na^+ ion. To maintain overall electrical neutrality, Dy^{3+} acts as a donor leading to some Na-site vacancies [Eq. (3), V'_{NA}] in the lattice, which can relax the strain caused by reorientation of domains. Therefore, the movement of the domains becomes easier and thus the piezoelectric properties of the BNBT6 ceramics are improved significantly [10]. The replacement of Bi^{3+} or Na^+ by Dy^{3+} makes a contribution to improve the piezoelectric properties. In addition, substitution by smaller ion Dy^{3+} causes compressive strain on the lattice with respect to octahedral unit in perovskite lattices, making to transform to rhombohedaral. As a result, it might lead to easy domain reorientation and make piezoelectric properties improved [37]. Furthermore, easier domain reorientation increases the degree of modulating spontaneous polarization, which makes the remnant polarization P_r increase. These results agree with the results in Fig. 5. However, if the amount of Dy_2O_3 is excessive, the distortion of crystal cell would be enlarged, the difficulty of polarization would be increased. As a result, the piezoelectric properties of BNBT6 ceramics doped with 0.8 wt.% Dy_2O_3 decreases subsequently.

Typically, large remnant polarization usually facilitates the piezoelectric properties of the piezoelectric ceramics. Compared with P_r of BNBT6 ceramics doped with 0.4 wt.% Dy_2O_3, P_r of BNBT6 ceramics doped with 0.6 wt.% Dy_2O_3 is lower, as shown in Fig. 5, but d_{33} is higher than that of BNBT6 ceramics doped with 0.4 wt.% Dy_2O_3. It's probably due to the lower E_c of 0.6 wt.% Dy_2O_3 doped BNBT6 ceramics, which makes the BNBT6 ceramics be prone to be polarized.

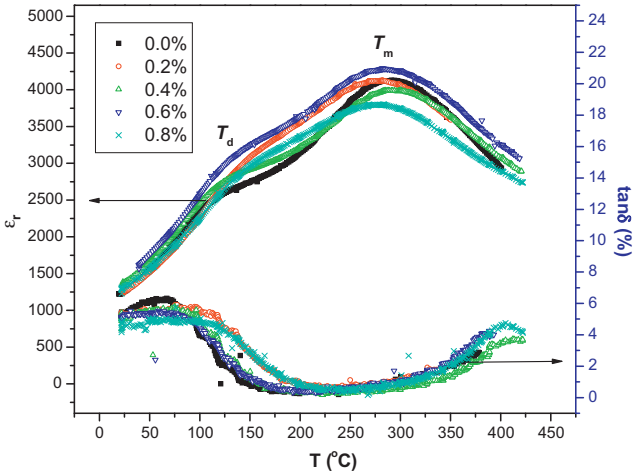

Fig. 6. Relative dielectric constants at a frequency of 10 kHz of BNBT6-x (wt.%) Dy_2O_3 ($x = 0.0$, 0.2, 0.4, 0.6 and 0.8) ceramics as a function of temperature.

According to the thermodynamic theory, d_{33} is correlated with the electrostriction coefficient Q_{11}, the spontaneous polarization P_s (which may be approximated by P_r) and relative permittivity ε_r via a general equation $d_{33} = 2Q_{11}\varepsilon_0\varepsilon_r P_s$, where ε_0 is the permittivity of free space. Q_{11} is related to the domain structure and should not change significantly by doping for the ceramics studied here [32,38]. Hence, the maximum d_{33} value observed for the BNBT6 ceramics doped with 0.6 wt.% Dy_2O_3 should also be attributed to the maximum ε_r as discussed in Fig. 6.

As a whole, compared with the pure BNBT6 ceramics, the mechanical quality factor Q_m of the BNBT6 ceramics doped with Dy_2O_3 decreases and Q_m is 102 at the doping level of 0.6 wt.%, as listed in Table 1. According to "soft" and "hard" additive model, Dy_2O_3 acts as a soft-additive and promotes the movement of the domains, leading to an increase of inner attrition together with a decrease of Q_m of modified BNBT6 ceramics compared with pure BNBT6 ceramics. Excessive Dy_2O_3 (0.8 wt.%) increases the difficulty of polarization, so inner attrition decreases and leads to the increase of Q_m again, as shown in Table 1.

Fig. 6 shows temperature dependence of relative dielectric constant and the loss tangent of BNBT6-x (wt.%) Dy_2O_3 ceramics at a frequency of 10 kHz. The curves of temperature dependence of relative dielectric constant for different samples look similar, which all shows two-phase transitions, as indicated in Fig. 6. T_d is the depolarization temperature which corresponds to the transition from a ferroelectric state to so-called "anti-ferroelectric" state which is defined as one in which lines of ions in the crystal are spontaneously polarized, but with neighboring lines polarized in antiparallel directions [39], while T_m is the maximum temperature at which relative dielectric constant ε_r reaches a maximum value and corresponds to a transition from an "anti-ferroelectric" state to a paraelectric state [40]. The Curie point (T_c) can be approximately determined by using the maximum temperature (T_m) [21]. From Fig. 6, the Dy_2O_3 addition induces an obvious decrease in T_c and increase of in T_d of the BNBT6 ceramics. At room temperature, the sample has higher relative dielectric constant: $\varepsilon_r = 1539$ when $x = 0.4$ and $\varepsilon_r = 1611$ when $x = 0.6$. Furthermore, compared with pure BNBT6 ceramics, the dielectric maxima become significantly higher at $x = 0.6$. It is 4127 for pure BNBT6 ceramics, 4291 for 0.6 wt.% Dy_2O_3 doped BNBT6 ceramics. However, the dielectric maxima becomes lower when the addition of Dy_2O_3 is super-

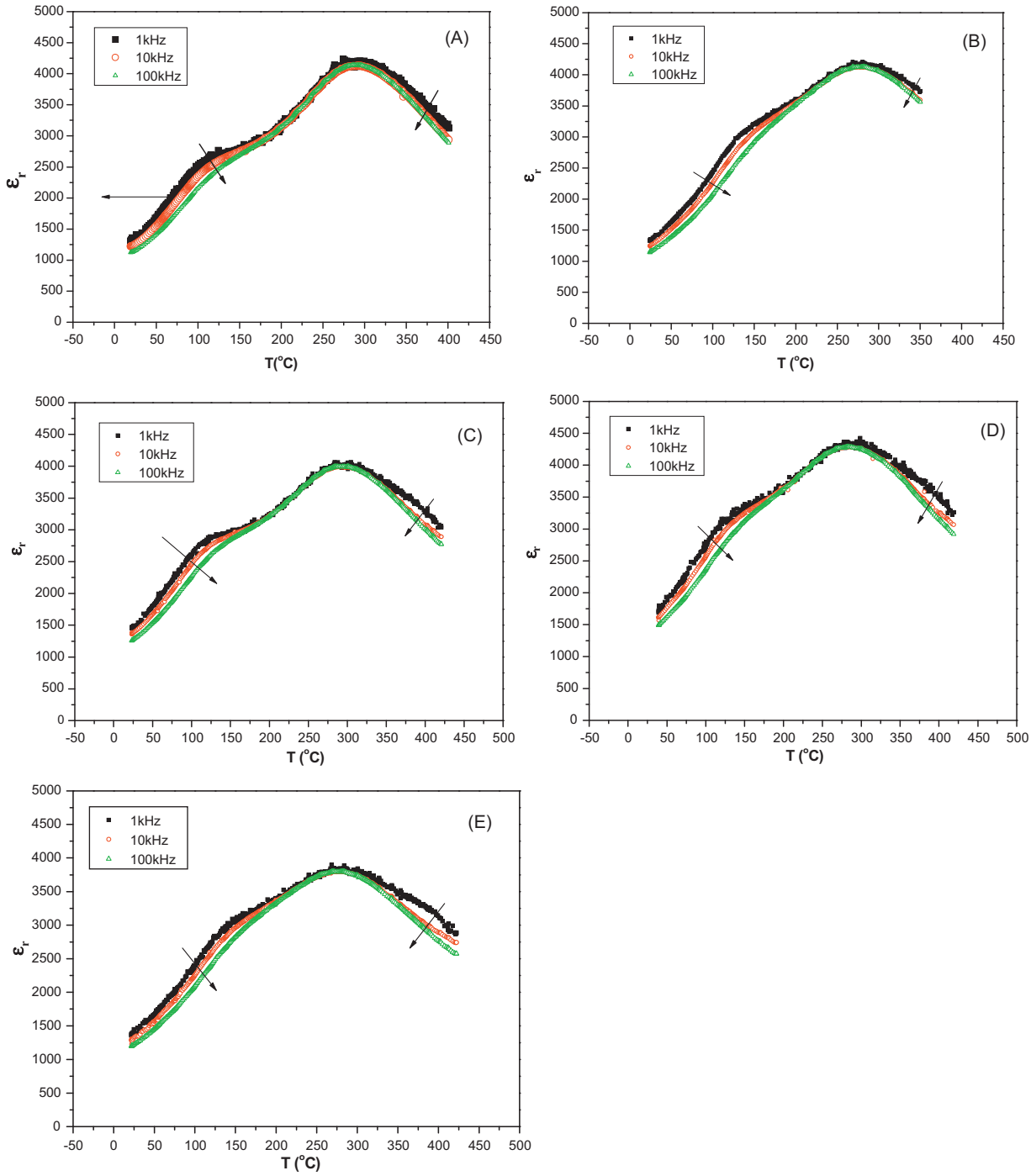

Fig. 7. Dielectric constants of BNBT6-x (wt.%) Dy_2O_3 ceramics as a function of temperature and frequency: (A) $x = 0.0$, (B) $x = 0.2$, (C) $x = 0.4$, (D) $x = 0.6$, (E) $x = 0.8$.

abundant ($x = 0.8$), suggesting that the dielectric properties are weakened when addition of Dy_2O_3 is superabundant.

From Fig. 6, it is found that the loss tangent $\tan\delta$ gradually increases with temperature up to T_d where it reaches its maximum due to the ferroelectric to anti-ferroelectric phase transition, and then decreases with the temperature because of the less distortion in the crystalline structure after depolarization until T_m [41,42]. Low dielectric loss at room temperature is obtained in all samples and it changes slightly with the increase of Dy_2O_3, and the ceramics doped with 0.6 wt.% Dy_2O_3 have a low dissipation factor ($\tan\delta = 0.051$) at a frequency of 10 kHz.

Fig. 7 shows temperature and frequency dependences of dielectric properties of BNBT6-x (wt.%) Dy_2O_3 ceramics. For each specimen, relative dielectric constant (ε_r) exhibit strong temperature–frequency dependence, indication of a typical relaxor ferroelectric behavior, as shown in Fig. 7. ε_r shows a very strong dependence on frequency below T_d, this dependence becoming weaker between T_d and T_m. However, the dependence becomes obvious again above T_m. This result is similar to Ref. [43]. With increasing frequency, dielectric constant of each specimen decreases. The value of the dielectric constant of each specimen at higher frequencies markedly dropped. This phenomenon can be explained in terms of interfacial polarization. The built-up of charges at the grain-grain boundary interface is responsible for large polarization, therefore, the high dielectric constant exists at lower frequencies [44]. Besides, T_d gradually shifts to a higher

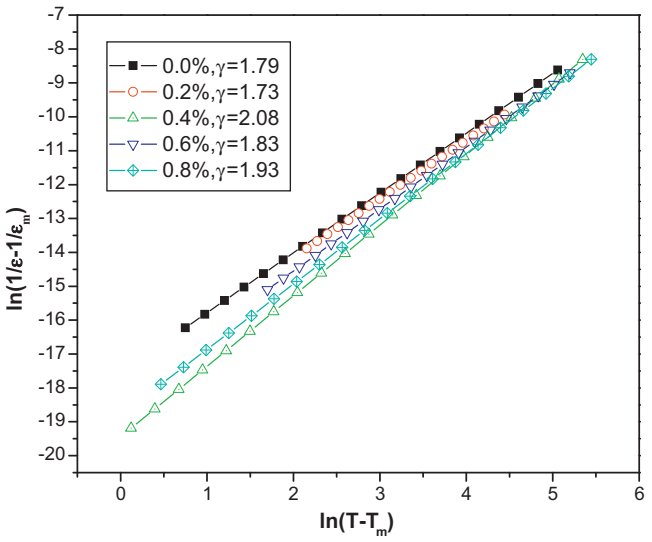

Fig. 8. Plots of $\ln(1/\varepsilon - 1/\varepsilon_m)$ as a function of $\ln(T - T_m)$ at 10 kHz for BNBT6-x (wt.%) Dy_2O_3 ceramics.

temperature with increasing frequency and T_m changes not much. The "shoulder" (T_d) becomes smaller with increasing frequency. All samples show similar dissipation factor behavior [15].

According to the theory of dielectric response of relaxor ferroelectrics discovered by Thomas [45], when the coupling reaction between A site cation and BO_6 octahedron decreases, the stability of ferroelectric domain decreases. Dy^{3+} occupying A site in BNBT6 lattice can create vacancy of A site, as discussed in Eq. (3). Moreover, the significant volatility of Bi^{3+} from the ceramics during high temperature sintering also creates A site vacancy. Therefore, the coupling reaction between A site and BO_6 octahedron is weakened, which leads to the relaxor characteristics in the ceramics [46]. Moreover, in the solid solution of BNBT6, Dy^{3+} ions occupy A-sites of ABO_3 perovskite structure, which may act as defects to destroy the long range ordering in the materials, therefore the ion disorder in the perovskite unit cell should be one of the reasons for the appearance of the frequency dispersion [47].

In order to characterize the dielectric dispersion and diffuseness of the phase transition, the modified Curie–Weiss law is proposed by many researchers [48–50]:

$$\frac{1}{\varepsilon} - \frac{1}{\varepsilon_m} = \frac{(T - T_m)^\gamma}{C} \quad (4)$$

where ε is dielectric constant at a temperature T and ε_m is its maximum value at T_m, C is a constant and γ is called the degree of relaxation which is used to express the diffuseness exponent of the phase transition. By fitting the experimental data based on Eq. (4), we obtain the value of parameter γ. The value of γ can vary from 1, for normal ferroelectrics with a normal Curie–Weiss behavior, to 2, for completely disordered relaxor ferroelectrics [51,52].

Fig. 8 shows the plot of $\ln(1/\varepsilon - 1/\varepsilon_m)$ as a function of $\ln(T - T_m)$ at 10 kHz for BNBT6-x (wt.%) Dy_2O_3 ceramics and the γ values of each specimen. It is obvious that the value of γ for all BNBT6 ceramics is close to 2, suggesting the appearance of the typical relaxor behavior. Moreover, the dielectric properties sensitively depend on the Dy_2O_3 content, the value of γ increases with the increasing Dy_2O_3 content and then decreases, the value of γ reaches peak values 2.08 at the doping level of 0.4 wt.% Dy_2O_3. This result indicates that a little Dy_2O_3 doped BNBT6 ceramics increases the degree of the relaxor behavior, and then the degree of the frequency dispersion weakens and the relaxor behavior decreases as the further Dy_2O_3 content (0.6–0.8 wt.%) increases.

4. Conclusions

The BNBT6 ceramics doped with 0–0.8 wt.% Dy_2O_3 has been investigated. No obvious change in the crystal structure is observed for BNBT6 ceramics doped with Dy_2O_3. The addition of appropriated Dy_2O_3 improves the piezoelectric and dielectric properties of BNBT6 ceramics significantly. At room temperature, the piezoelectric constant d_{33} and planar coupling factor k_p reaches peak values at the doping level of 0.6 wt.% and 0.4 wt.% Dy_2O_3 respectively: d_{33} = 170 pC/N, k_p = 0.33, the mechanical quality factor Q_m is 102, ε_r attains 1611 and $\tan\delta$ = 0.051 (at a frequency of 10 kHz) at the Dy_2O_3 doping level of 0.6 wt.%. The P–E hysteresis loops on BNBT6-x (wt.%) ceramics show that the proper Dy_2O_3 addition results in the increase of the remnant polarization P_r and the decrease of the coercive field E_c, and then more loop squareness are obtained with increasing Dy_2O_3 contents, and R_{sq} reaches a peak value 1.40 at x = 0.2. Moreover, the BNBT6 ceramics doped with Dy_2O_3 have the ferroelectric relaxor behavior and the degree of the relaxor behavior attains peak value (γ = 2.08) at the doping level of 0.4 wt.%.

Acknowledgements

This work was supported by National Nature Science Foundation of China (Nos. 50602021 and 50802038) and School Foundation of LCU.

References

[1] B. Jaffe, W. Cook, H. Jaffe, Piezoelectric Ceramics, Academic, New York, 1971, pp. 185–212.
[2] J.H. Yoo, K.H. Yoo, Y.W. Lee, S.S. Suh, J.S. Kim, C.S. Yoo, Jpn. J. Appl. Phys. 39 (2000) 2680–2684.
[3] Y.J. Zhang, R.Q. Chu, Z.J. Xu, J.G. Hao, Q. Chen, P. Fu, W. Li, G.R. Li, Q.R. Yin, J. Alloys Compd. 502 (2010) 341–345.
[4] Y.M. Li, W. Chen, Q. Xu, J. Zhou, Y. Wang, H.J. Sun, Ceram. Int. 33 (2007) 95–99.
[5] T. Takenaka, H. Nagata, J. Eur. Ceram. Soc. 25 (2005) 2693–2700.
[6] H.E. Mgbemere, R.P. Herber, G.A. Schneider, J. Eur. Ceram. Soc. 29 (2009) 1729–1733.
[7] D.M. Lin, K.W. Kwok, Curr. Appl. Phys. 10 (2010) 422–427.
[8] Y.M. Li, W. Chen, Q. Xu, J. Zhou, X.Y. Gu, Mater. Lett. 59 (2005) 1361–1364.
[9] C.E. Peng, J.F. Li, W. Gong, Mater. Lett. 59 (2005) 1576–1580.
[10] Z.W. Chen, J.Q. Hu, Ceram. Int. 35 (2009) 111–115.
[11] C.R. Zhou, X.Y. Liu, W.Z. Li, C.L. Yuan, J. Phys. Chem. Solids 70 (2009) 541–545.
[12] D.Z. Zhang, X.J. Zhenga, X. Feng, T. Zhang, J. Sun, S.H. Dai, L.J. Gong, Y.Q. Gong, L. He, Z. Zhu, J. Huang, X. Xu, J. Alloys Compd. 504 (2010) 129–133.
[13] C. Ma, X. Tan, Solid State Commun. 150 (2010) 1497–1500.
[14] W.C. Lee, C.Y. Huang, L.K. Tsao, Y.C. Wu, J. Alloys Compd. 492 (2010) 307–312.
[15] Z.P. Yang, B. Liu, L.L. Wei, Y.T. Hou, Mater. Res. Bull. 43 (2008) 81–89.
[16] D.M. Lin, K.W. Kwok, H.L.W. Chan, J. Alloys Compd. 481 (2009) 310–315.
[17] Z.P. Yang, Y.T. Hou, H. Pan, Y.F. Chang, J. Alloys Compd. 480 (2009) 246–253.
[18] M.J. Zou, H.Q. Fan, L. Chen, W.W. Yang, J. Alloys Compd. 495 (2010) 280–283.
[19] M.L. Liu, D.A. Yang, Y.F. Qu, J. Alloys Compd. 496 (2010) 449–453.
[20] T. Takenaka, K. Maruyama, K. Sakata, Jpn. J. Appl. Phys. 30 (1991) 2236–2239.
[21] M. Chen, Q. Xu, B.H. Kim, B.K. Ahn, J. Eur. Ceram. Soc. 28 (2008) 843–849.
[22] B.J. Chu, D.R. Chen, G.R. Li, J. Eur. Ceram. Soc. 22 (2002) 2115–2121.
[23] H.L. Du, W.C. Zhou, F. Luo, D.M. Zhu, Appl. Phys. Lett. 91 (2007) 202907.
[24] D.M. Lin, K.W. Kwok, H.W.L. Chan, Appl. Phys. Lett. 91 (2007) 143513.
[25] G.F. Fan, W.Z. Lu, X.H. Wang, F. Liang, Appl. Phys. Lett. 91 (2007) 202908.
[26] L.J. Liu, H.Q. Fan, S.M. Ke, X.L. Chen, J. Alloys Compd. 458 (2008) 504–508.
[27] J.H. Shi, W.M. Yang, J. Alloys Compd. 472 (2009) 267–270.
[28] X.X. Wang, H.L.W. Chan, C.L. Choy, Solid State Commun. 125 (2003) 395–399.
[29] C.R. Zhou, X.Y. Liu, W.Z. Li, Mater. Res. Bull. 44 (2009) 724–727.
[30] P. Fu, Z.J. Xu, R.Q. Chu, W. Li, G.Z. Zang, J.G. Hao, Mater. Des. 31 (2010) 796–801.
[31] Q. Xu, M. Chen, W. Chen, H.X. Liu, Acta Mater. 56 (2008) 642–650.
[32] D.M. Lin, K.W. Kwok, H.L.W. Chan, Appl. Phys. 40 (2007) 6778–6783.
[33] J. Shieh, K.C. Wu, C.S. Chen, Acta Mater. 55 (2007) 3081–3087.
[34] S. Wongsaenmai, S. Ananta, R. Yimnirun, J. Alloys Compd. 474 (2009) 241–245.
[35] H.D. Li, C.D. Feng, W.L. Yao, Mater. Lett. 58 (2004) 1194–1198.
[36] S.R. Georges, B.K. Mukherjee, R. Wei, G.M. Yang, J. Appl. Phys. 101 (2007) 064111.
[37] P. Fu, Z.J. Xu, R.Q. Chu, W. Li, G.Z. Zang, J.G. Hao, Mater. Sci. Eng. B 167 (2010) 161–166.
[38] D.M. Lin, K.W. Kwok, Curr. Appl. Phys. 10 (2010) 1196–1202.
[39] C. Kittel, Phys. Rev. 82 (1951) 729–732.
[40] C.G. Xu, D.M. Lin, K.W. Kwok, Solid State Sci. 10 (2008) 934–940.
[41] K. Sakata, T. Takenaka, Y. Naitou, Ferroelectrics 131 (1992) 219–226.

[42] Y.W. Liao, D.Q. Xiao, D.M. Lin, J.G. Zhu, P. Yu, L. Wu, X.P. Wang, Ceram. Int. 33 (2007) 1445–1448.
[43] Z.P. Yang, Y.T. Hou, B. Liu, L.L. Wei, Ceram. Int. 35 (2009) 1423–1427.
[44] Z.H. Yao, H.X. Liu, Y. Liu, Z.H. Wu, Z.Y. Shen, Y. Liu, M.H. Cao, Mater. Chem. Phys. 109 (2008) 475–481.
[45] N.W. Thomas, J. Phys. Chem. Solids 51 (1990) 1419.
[46] C.R. Zhou, X.Y. Liu, W.Z. Li, C.L. Yuan, G.H. Chen, Curr. Appl. Phys. 10 (2010) 93–98.
[47] J.G. Hao, Z.J. Xu, R.Q. Chu, G.Z. Zang, G.R. Li, J. Alloys Compd. 484 (2009) 233–238.
[48] X.J. Chou, J.W. Zhai, X. Yao, Mater. Chem. Phys. 109 (2008) 125–130.
[49] L. Khemakhem, A. Kabadou, A. Maalej, A.B. Salah, A. Simon, M. Maglione, J. Alloys Compd. 452 (2008) 451–455.
[50] S. Senda, J.P. Mercurio, J. Eur. Ceram. Soc. 21 (2001) 1333–1336.
[51] D. Viehland, M. Wuttig, L.E. Cross, Ferroelectrics 76 (1987) 241–267.
[52] W. Supatrra, X.L. Tan, A. Supon, Y. Rattikorn, J. Alloys Compd. 454 (2008) 331–339.